A CMIP6 ensemble for downscaled monthly climate normals over North America

Colin R. Mahony[1]*, Tongli Wang[2], Andreas Hamann[3], and Alex Cannon[4]

1. British Columbia Ministry of Forests, Lands, Natural Resource Operations and Rural Development, Victoria, BC, Canada.
2. Centre for Forest Conservation Genetics, Department of Forest and Conservation Sciences, Faculty of Forestry, University of British Columbia, Canada
3. Department of Renewable Resources, Faculty of Agricultural, Life, and Environmental Sciences, University of Alberta, Canada
4. Climate Research Division, Environment and Climate Change Canada, Victoria, British Columbia, Canada

*Correspondence to colin.mahony@gov.bc.ca; twitter @ColinRMahony

Abstract

Many studies of climate change impacts and adaptation use climate model projections downscaled at very high spatial resolution (~1km) but very low temporal resolution (20- to 30-year normals). These applications have model selection priorities that are distinct from analyses at high temporal resolution. Here, we select a 13-model CMIP6 ensemble designed for robust change-factor downscaling of monthly climate normals and describe its attributes in North America. The ensemble is representative of the distribution of equilibrium climate sensitivity and grid resolution in the CMIP6 generation. We provide rationale for a 9-member subset of the ensemble based on screening criteria and sequence these 9 models for selection of smaller ensembles for regional analysis. Although we have focused our documentation on North America, the 13-model ensemble is selected using global criteria and applicable to downscaling climate normals in other continents.

1. Introduction

The most recent iteration of the Coupled Model Intercomparison Project (CMIP6; Eyring et al. 2016) is a once-in-a-decade update to projections of climate change. CMIP6 provides a larger number of simulations from a new generation of global climate models, at higher spatial resolution, and using an improved set of emissions scenarios relative to its predecessor, CMIP5 (Taylor et al. 2012). These new climate simulations contribute to and are put into broader context by the Sixth Assessment Report from Working Group I of the Intergovernmental Panel on Climate Change. CMIP6 simulations are rapidly being incorporated into downscaled climate data products for use in regional climate change impacts and adaptation initiatives. These initiatives can benefit from careful selection of climate model projections that are suited to broad classes of end uses, and from greater transparency on the attributes of these ensembles.

Many climate change impact analyses, particularly in ecology, use projections of climate change that are downscaled to very high resolution (~1km) but very low temporal resolution (20-30 year climate normals). The prevalence of this type of analysis is evident from the widespread use of WorldClim (Hijmans et al. 2005, Fick and Hijmans 2017; 23340 citations) and ClimateNA (Wang et al. 2012, 2016, Hamann et al. 2013; 1678 citations). The low temporal resolution of these applications simplifies downscaling; both WorldClim and ClimateNA use change-factor downscaling, also called simple mean bias correction (Maraun 2016). This method adds low-spatial-resolution anomalies from the climate model to a high-resolution gridded climate map (Tabor and Williams 2010). The best practices for change-factor downscaling to high-spatial and low-temporal resolution are different than those for more sophisticated statistical downscaling techniques required for high temporal resolution downscaling (Wilby et al. 2004), leading to distinct model selection priorities.

One consideration in model selection for change-factor downscaling is the number of simulation runs for each candidate model. The change-factor method is sensitive to the influence of natural variability in the historical reference period against which anomalies are calculated and bias correction is applied. Similarly, natural variability during the projected future periods adds “noise” to the climate change “signal”, the latter being of primary interest to analyses of projected climate normals. Performing change-factor downscaling with multiple simulations runs of each model reduces the confounding influence of natural variability in bias correction and improves the signal-to-noise ratio. Models with multiple simulations for each historical and future scenario are preferable in this context.

Another consideration is the model bias. All climate models exhibit biases--systematic differences between observations and simulations—at the regional scale. Removal of these biases is a basic step in downscaling (Maraun 2016). Change-factor downscaling performs univariate bias correction and therefore does not conserve the physical (e.g., thermodynamic) interdependence between variables such as temperature and precipitation (Cannon 2018). The associated potential for univariate downscaling to produce physically implausible climatic conditions presumably increases with the size of the biases in the simulation. For this reason, models with small biases are preferable to models with large biases, all else being equal.

Finally, the spatial resolution of climate models is of interest to high spatial resolution downscaling. Some models contributing to the CMIP6 ScenarioMIP experiment (the candidate pool for ensemble selection in this study) have horizontal grid resolutions of 70-100km. These medium-resolution models are able to resolve macrotopography, e.g., to differentiate the major mountain ranges of the Western Cordillera. The opportunity to better represent the influences of water bodies and topography on climate change trends, such as elevation-dependent warming (Palazzi et al. 2019), is appealing for climate change impact analyses. Nevertheless, medium-resolution models may bring new challenges for high-resolution change-factor downscaling. Conversely, models with very low spatial resolution (>300km) can conflate the climate change signals of distinct regions, particularly at land/ocean transitions. Very low resolution therefore is a consideration for exclusion from ensembles designed for high-resolution change-factor downscaling.

Collectively, the three considerations described above suggest an ensemble that prioritizes number of simulations per model rather than number of models, low-to-moderate bias, and moderate-to-high spatial resolution.

Once a general-purpose ensemble is selected, it is useful to structure the ensemble for further user-specific model selection. Many applications of projected climate normals are computationally intensive analyses at regional scales. In these cases, it is often desirable to use a small number (3-8) of models that represent the approximate range of a more comprehensive ensemble. Cannon (2015) describes a method for structuring an ensemble into an order of subset selection that optimally represents the ensemble spread. Alternatively, analysts may wish to select a custom subset of the ensemble. Documentation of the attributes of the ensemble members can help analysts to identify subsets that are best suited to specific applications.

The purpose of this study is to document and characterize an ensemble of CMIP6 model projections of 21st century climate change over North America for use in ClimateNA (Wang et al. 2016; http://climatena.ca/). The focus of model selection is on facilitating robust downscaling of climate normals at high spatial resolution and low temporal resolution. We characterize the attributes, biases, and climate change trends of the ensemble and highlight features of interest in individual climate models. Finally, we provide ordered subsets of the ensemble for regional analyses and considerations for selection of custom subsets. This information is complemented by an interactive web application to explore the ensemble in more detail (https://bcgov-env.shinyapps.io/cmip6-NA/).

2. Methods

2.1. Criteria for model selection

We assessed all models in the ESGF holdings for the CMIP6 ScenarioMIP as of December 15, 2020. We selected models using six objective criteria, listed below with rationale:

- **Criterion 1: T_{min} and T_{max} available.** Mean daily minimum temperature (T_{min}) and mean daily maximum temperature (T_{max}) are the directly measured elements of the long-term temperature record, and are essential to the downscaling and variable derivation in ClimateNA.

- **Criterion 2: Minimum of 3 historical runs available.** This criterion ensures robust downscaling by reducing the confounding influence of natural variability in bias correction.

- **Criterion 3. Complete scenarios.** Models need to have at least one simulation for three of the four major SSP marker scenarios (SSP1-2.6, SSP2-4.5, SSP3-7.0, and SSP5-8.5).

- **Criterion 4. One model per institution.** This criterion is a widely applied best practice in ensemble selection (Leduc et al. 2016) as one measure to increase independence among ensemble members. For the purposes of this criterion, different physics or forcing schemes of the same model were considered different models.

- **Criterion 5. No closely related models.** Models that share components were excluded, following Figure 5 of Brunner et al. (2019).

- **Criterion 6. No large biases.** Bias is the degree to which a model simulation differs from the observed climate over a reference period (1961-1990 in this case). Models with much larger biases than the rest of the ensemble in one or more variables were excluded.

2.2. Analysis of model bias

We assessed model bias as *mean absolute bias* over North America in each monthly climate variable. For each grid cell, *i*, the mean simulated 1961-1990 climate normal of the *K* historical model runs, f_{ik} is calculated as

$$\bar{f_i} = \frac{1}{K}\sum_{k=1}^{K} f_{ik} \qquad (1)$$

The absolute value of the difference between the simulated 1961-1990 normal, $\bar{f_i}$, and the observed 1961-1990 normal, o_i, aggregated onto the native model grid is calculated for each grid cell:

$$|e_i| = |\bar{f_i} - o_i| \qquad (2)$$

The mean absolute bias, $|e|$, over all *N* projected grid cells in North America is calculated as:

$$|e| = \frac{1}{N}\sum_{i=1}^{N} |e_i| \qquad (3)$$

To equalize the area of grid cells, we projected absolute bias in the native model grid onto a Lambert Conformal Conic grid with 0.5^{o} resolution prior to calculating this mean.

For precipitation variables, Equations 1 and 2 were performed on log-transformed normals. Following Equation 3, this log-transformation was reversed by taking the exponent of absolute bias. Doing so expresses absolute bias of precipitation as a factor of magnitude. e.g., simulated precipitation of 50% and 200% relative to observed precipitation both have an absolute bias of 2.

2.3. Ensemble subset criteria

Users of the ensemble may wish or need to use a lesser number of models in their analyses. To support the selection of subsets, we structure the ensemble by defining an order of exclusion of models. Models are excluded in two phases: first based on screening criteria to exclude models with lower value for the anticipated uses of the ensemble, and second using the method of Cannon (2015) to best represent the range of climate changes in the remaining models.

2.3.1. Screening criteria

Priority for exclusion from model subsets was established using four screening criteria. The screening criteria are more subjective than the six selection criteria defined above. They generally are not sufficient in isolation but combinations of the criteria provide some justification for model exclusions.

- **Criterion 7. Constraints on equilibrium climate sensitivity (ECS).** Multiple lines of evidence indicate that the Earth's equilibrium climate sensitivity (ECS) is very likely between 2^{o}C and 5^{o}C (Liang et al. 2020, Sherwood et al. 2020, Tokarska et al. 2020). The evidence is robust for the lower bound, and weaker for the upper bound. From one perspective, inclusion of models with ECS outside this range unnecessarily increases the modeling uncertainty in downstream analyses. The opposing perspective is that high-sensitivity models are useful as a representation of high-impact, low-likelihood scenarios (Sutton and Hawkins 2020). To accommodate both perspectives, we provide structured subsets with and without high-sensitivity models.

- **Criterion 8. Model resolution.** Some ScenarioMIP models have sufficiently high spatial resolution to resolve macrotopography, e.g., to differentiate the major mountain ranges of the Western Cordillera. These models are weighted towards inclusion in the ordered subsets. Models with very low spatial resolution are weighted towards exclusion in the subset.

- **Criterion 9. Number of simulation runs.** The ensemble is designed for analysis of projected climate normals; the climate change signal is of primary interest. In this context, internal variability of the models is a confounding factor, producing erratic climate change trajectories in noisy climate variables like precipitation and winter temperature. The signal-to-noise ratio can be increased by averaging the projected normals over multiple simulations of the same emissions scenario. Models with only one run are weighted for exclusion.

- **Criterion 10: Grid cell artefacts.** Models exhibiting spatially anomalous climate changes in individual grid cells are problematic for many of the intended uses of this ensemble, and are weighted for exclusion from the structured subsets.

2.3.2. Ordered subsets

After exclusion of models using the screening criteria above, an order of exclusion for the remaining models is defined using the Katsavounidis–Kuo–Zhang (KKZ) algorithm, using the application to climate model ensemble selection described by Cannon (2015). KKZ deterministically selects models that best represent the spread of multivariate climate changes projected by the ensemble. KKZ subset selection is ordered, starting with the model closest to the ensemble centroid, and incrementally adding models to a region of the ensemble variation that is poorly represented by each successive subset.

Since the spatial patterns of climate change differ among models, we provide separate KKZ subsets for each of the 7 IPCC climate reference regions (Iturbide et al. 2020) within North America. We do not provide an ordered subset for North America as a whole, given that ensembles of <9 models are insufficient to represent spatial variation in modeling uncertainty at continental scales (Pierce et al. 2009, McSweeney et al. 2014, Cannon 2015). The implementation of KKZ in this study used the mean of the z-standardized seasonal changes in T_{min}, T_{max}, and precipitation in four consecutive 20-year time periods starting with 2021-2040 and three emissions scenarios (SSP1-2.6, SSP2-4.5, and SSP3-7.0).

3. Results

3.1. Ensemble selection

There were 44 models in the CMIP6 ScenarioMIP holdings as of December 15, 2020 (Table 1). Twelve of these candidates were excluded because they did not provide monthly means of T_{min} and T_{max} (Criterion 1). Notably, CESM2 does provide T_{min} and T_{max} in its future projections, but due to an archiving error these variables are not available for historical runs. An additional eleven models were excluded because they had less than three historical runs (Criterion 2) or an incomplete scenario set (Criterion 3). Of the 21 models that passed these first three strict criteria, we excluded two more models on the basis of having a clear choice between models from the same institution (Criterion 4): CanESM5-CanOE in favour of CanESM5; and EC-Earth3-Veg in favour of EC-Earth3. In addition, of the several variants of the GISS-E2-1-G model, we selected the r*i1p3f1 variant because it had the most complete set of scenario simulations. We downloaded historical simulations from the remaining 19 models for further evaluation. For practical purposes, we limited downloads to 5 historical simulations for EC-Earth3 due to its very high resolution and archiving structure, and 10 simulations for other models.

To assist with choosing among models from the same institution (Criterion 4) or with shared components (Criterion 5), we conducted an analysis of bias in T_{min}, T_{max}, and precipitation (PPT) (Figure 1). We excluded AWI-CM-1-1-MR on the sole basis of its very high temperature bias (Criterion 6). NESM3 also has high bias relative to the other models, and excluded due to shared components with MPI-ESM1 (Criterion 5). None of the other related models were distinct from each other in terms of bias.

Final choices from among related models were: UKESM1-0-LL selected over HadGEM3-GC31-LL due to higher resolution and more simulations; MIROC6 over MIROC-ES2L due to higher number of runs and regionally high biases in the Pacific Northwest. MPI-ESM1-2-HR over MPI-ESM1-2-LR to improve representation of high-resolution models in the ensemble; and CNRM-ESM2-1 arbitrarily selected over CNRM-CM6-1 in favour of the ESM configuration. In summary, the six criteria reduced the 44 candidate models to a 13-model ensemble.

Table 1: Candidate models, model exclusion criteria, and number of simulation runs. Model list and number of simulations per scenario are ESGF holdings as of December 15, 2020. ECS is equilibrium climate sensitivity (long-term temperature change in response to an instant doubling of CO2); ECS values are quoted from Meehl et al. (2020).

				ESGF holdings					Analyzed				
Model	**Criterion for exclusion**		**ECS**	historical	ssp126	ssp245	ssp370	ssp585	historical	ssp126	ssp245	ssp370	ssp585
ACCESS-CM2	2	<3 historical runs	4.7	**2**	1	1	1	1					
ACCESS-ESM1-5			3.9	**30**	10	30	10	10	**10**	10	10	10	10
AWI-CM-1-1-MR	6	very high bias	3.2	**5**	1	1	5	1	**3**				
BCC-CSM2-MR			3.3	**3**	1	1	1	1	**3**	1	1	1	1
CAMS-CSM1-0	1	No tmax/tmin	2.3	**3**	2	2	2	2					
CESM2	1	No tmax/tmin in historical	5.2	**11**	3	3	3	3					
CESM2-WACCM	1	No tmax/tmin in historical	4.8	**3**	1	5	3	5					
CIESM	3	incomplete scenarios		**3**	1			1					
CMCC-CM2-SR5	1	No tmax/tmin		**1**	1	1	1	1					
CNRM-CM6-1	4	same institution	4.9	**30**	6	10	6	6	**10**				
CNRM-CM6-1-HR	2	<3 historical runs	4.3	**1**	1	1	1	1					
CNRM-ESM2-1			4.8	**11**	5	10	5	5	**11**	5	5	5	5
CanESM5			5.6	**65**	50	50	50	50	**10**	10	10	10	10
CanESM5-CanOE	4	same institution		**3**	3	3	3	3					
E3SM-1-1	3	incomplete scenarios	5.3	**1**				1					
EC-Earth3			4.3	**73**	7	30	7	58	**5**	5	5	5	5
EC-Earth3-AerChem	2	<3 historical runs		**2**			1						
EC-Earth3-Veg	4	same institution	4.3	**8**	7	8	6	6					
FGOALS-f3-L	1	No tmax/tmin	3	**3**	3	3	3	3					
FGOALS-g3	1	No tmax/tmin	2.9	**6**	4	4	5	4					
FIO-ESM-2-0	3	incomplete scenarios		**3**	3	3		3					
GFDL-CM4	3	incomplete scenarios	3.9	**1**		1		1					
GFDL-ESM4			2.7	**3**	1	3	1	1	**3**	1	3	1	1
GISS-E2-1-G		selected r*i1p3f1 variants	2.7	**47**	7	30	19	7	**4**	4	4	4	4
HadGEM3-GC31-LL	5	shared components (UKESM1)	5.6	**5**	1	4		4	**4**				
HadGEM3-GC31-MM	3	incomplete scenarios	5.4	**4**	1			4					
IITM-ESM	1	No tmax/tmin		**1**	1	1	1	1					
INM-CM4-8	2	<3 historical runs	1.8	**1**	1	1	1	1					
INM-CM5-0			1.9	**9**	1	1	5	1	**9**	1	1	5	1
IPSL-CM6A-LR			4.6	**9**	5	6	9	5	**9**	5	6	9	5
KACE-1-0-G	1	No tmax/tmin		**3**	3	3	3	3					
KIOST-ESM	2	<3 historical runs		**1**	1	1		1					
MCM-UA-1-0	1	No tmax/tmin		**2**	1	1	1	1					
MIROC-ES2L	4	same institution	2.7	**3**	3	3	3	3	**3**				
MIROC6			2.6	**50**	50	50	3	50	**10**	10	10	3	10
MPI-ESM-1-2-HAM	3	incomplete scenarios		**3**			2						
MPI-ESM1-2-HR			3	**10**	2	2	10	2	**8**	2	2	10	1
MPI-ESM1-2-LR	4	same institution	3	**10**	10	10	10	10	**10**				
MRI-ESM2-0			3.1	**7**	1	5	5	2	**5**	1	5	1	1
NESM3	5	shared components (MPI-ESM1)	4.8	**5**	2	2		2	**5**				
NorESM2-LM	1	No tmax/tmin	2.6	**3**	1	3	3	1					
NorESM2-MM	1	No tmax/tmin	2.5	**1**	1	2	1	1					
TaiESM1	1	No tmax/tmin	4.4	**2**	1	1	1	1					
UKESM1-0-LL			5.4	**19**	16	17	16	5	**10**	5	5	5	5

3.2. Attributes of the 13-model ensemble

3.2.1. Representation of the full CMIP6 ensemble

The 13-model ensemble has a mean global equilibrium climate sensitivity (ECS) of 3.7°C and a range of 1.9-5.6°C, which matches ECS of the full CMIP6 ensemble (3.7°C; 1.8-5.6°C) (Meehl et al. 2020).

3.2.2. Model bias

The ensemble mean has a mean absolute bias of 2°C in T_{min} and T_{max}. Most models have biases similar to this baseline. However, AWI-CM-1-1-MR has exceptionally high bias in both T_{min} and T_{max}. ACCESS-ESM1-5, MIROC6, MIROC-ES2L and NESM3 also have high biases in T_{min} and/or T_{max}. There is less differentiation in precipitation biases among models and with the ensemble mean.

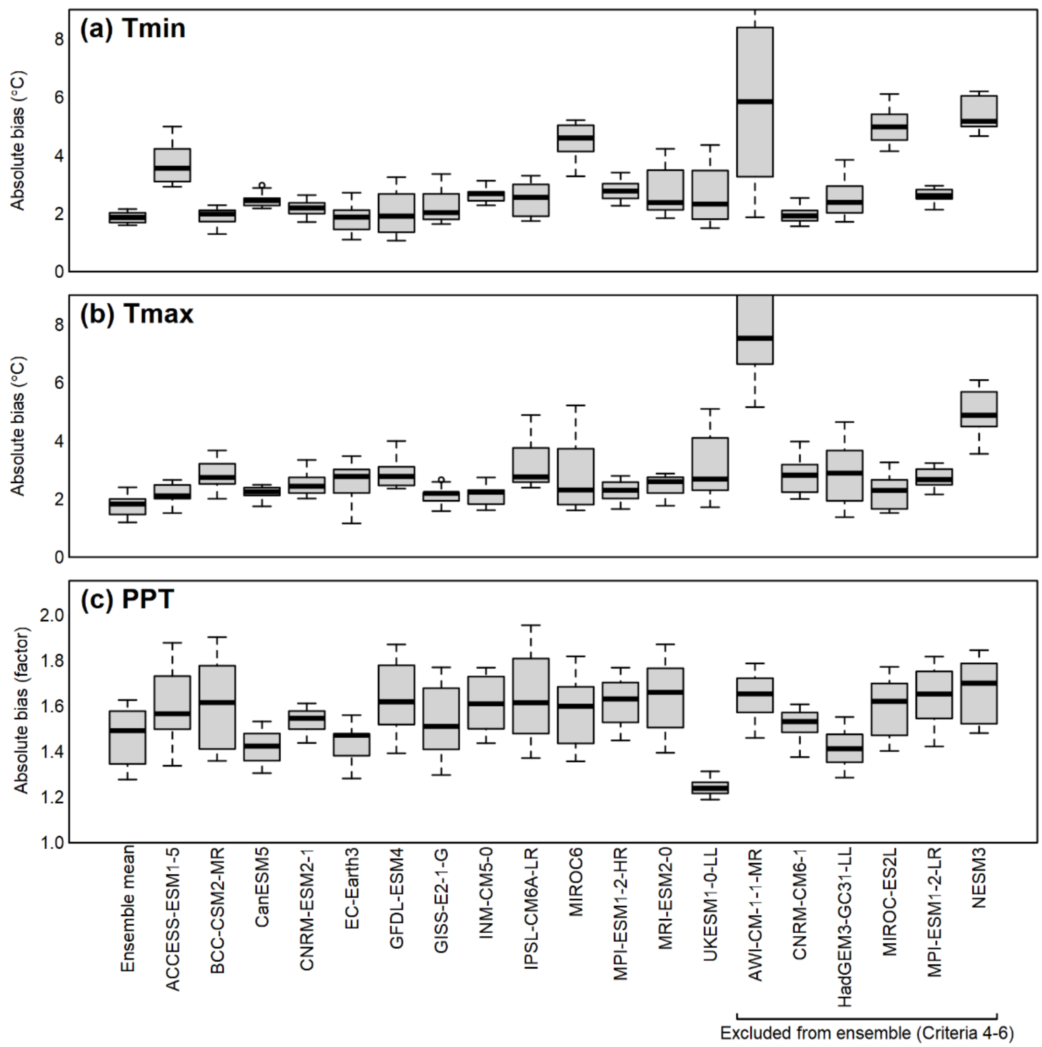

Figure 1: Model biases in monthly means of (a) daily minimum temperature, (b) daily maximum temperature, and (c) precipitation. Each box represents 12 values of mean absolute bias over North America, one for each month. Absolute bias for precipitation is expressed as a factor of magnitude, e.g., relative biases of 50% and 200% both have an absolute bias of 2.

3.2.3. Spatial resolution and model orography

The selected 13-model ensemble has a mean latitudinal grid resolution of 1.4° (range of 0.7°-2.8°) (Figure 2). Four models (EC-Earth3, GFDL-ESM4, MPI-ESM1-2-HR, and MRI-ESM2-0) resolve the macrotopography of the Western Cordillera, namely the Sierra Nevada, Cascade Range, Rocky Mountains, and British Columbia Coast Ranges. BCC-CSM2-MR does not resolve these ranges, despite having sufficient grid resolution to do so. CanESM5 has a very low resolution of 2.8°x2.8°.

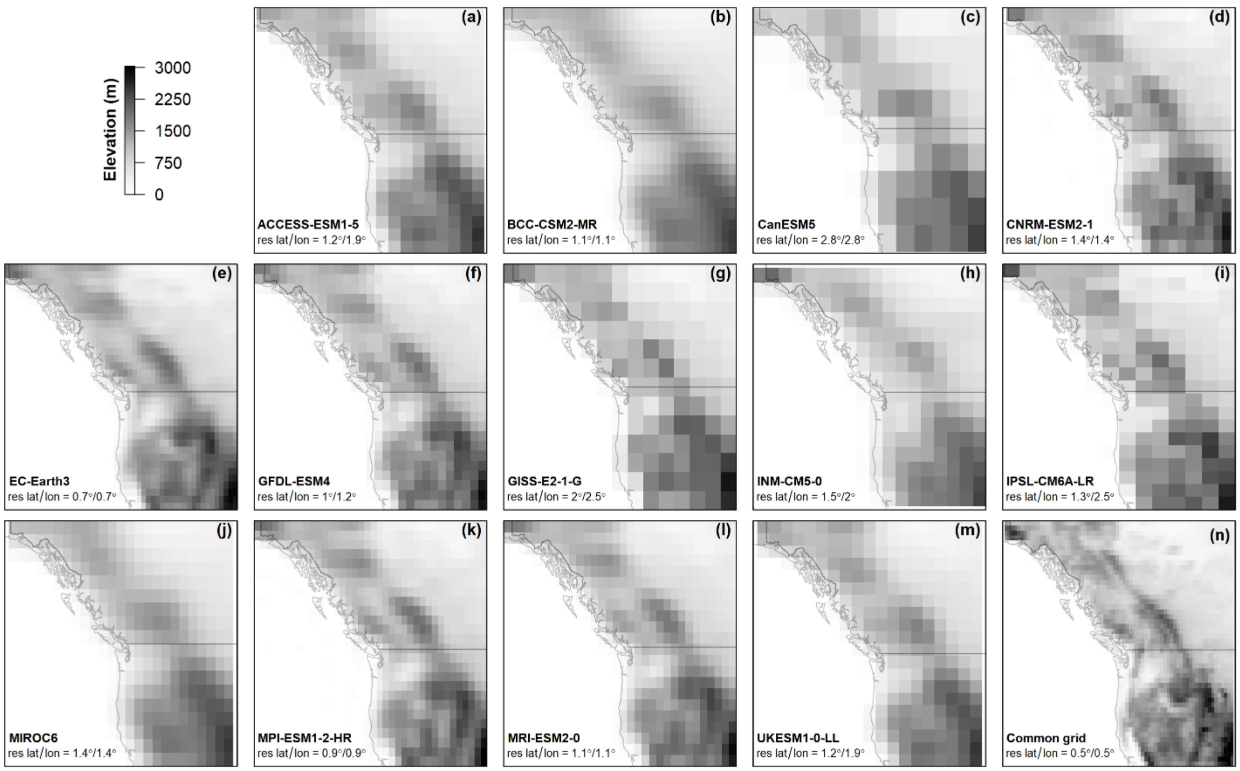

Figure 2: Effective topographic resolution of the 13 selected models. (a-m) model orography (elevation of land surface) in the native grid of each model. The extent of the map is central-western North America (106-142W, 37-62N). The common grid (panel n) is the 0.5° grid used for extraction of observations from ClimateNA.

3.2.4. Projected climate changes

A visual comparison of projected seasonal changes in T_{min}, T_{max}, and PPT (Figure 3) indicates some basic attributes of the ensemble simulations. All models exhibit arctic amplification of winter temperatures, though it is relatively subtle in EC-Earth3. Most models project the strongest summer warming at mid-latitudes. All models, with the exception of UKESM1, have a similar pattern of warming in T_{min} and T_{max}, though the magnitude of warming is greater for T_{min} in most models.

Continental-scale patterns of winter (Dec-Feb) precipitation change are somewhat consistent among models, with declines in Mexico and increases in the arctic regions. Deviations from this pattern are strongest in models with few (1-3) historical runs for SSP2-4.5 (BCC-CSM2-MR, GFDL-ESM4 and INM-CM5-0), and are likely due to internal variability. This result indicates the benefit of multiple runs in smoothing out natural variability to reveal the anthropogenic climate change signal in noisy climate variables like precipitation and winter temperature.

Most models project a reduction in summer (Jun-Aug) precipitation in the coastal areas of the Pacific Northwest (California, Oregon, Washington, and southern British Columbia). However, there is substantial disagreement among models in summer precipitation change over the rest of the continent. The muted summer precipitation change in the ensemble mean hides this ensemble disagreement, and underscores the importance of assessing climate change impacts with an ensemble of model projections rather than solely using the ensemble mean.

The two high-ECS models CanESM5 and UKESM1 have similar patterns and magnitudes of change in winter temperature and precipitation. However, they differ substantially in the summer, with UKESM1 showing much higher increases in daytime temperatures (T_{max}) in temperate and Boreal regions and stronger declines in precipitation in central North America. Although CanESM5 has a higher ECS and stronger trend in 1970-2014 global heating (Liang et al. 2020), UKESM1 projects stronger mid-century heating over North America.

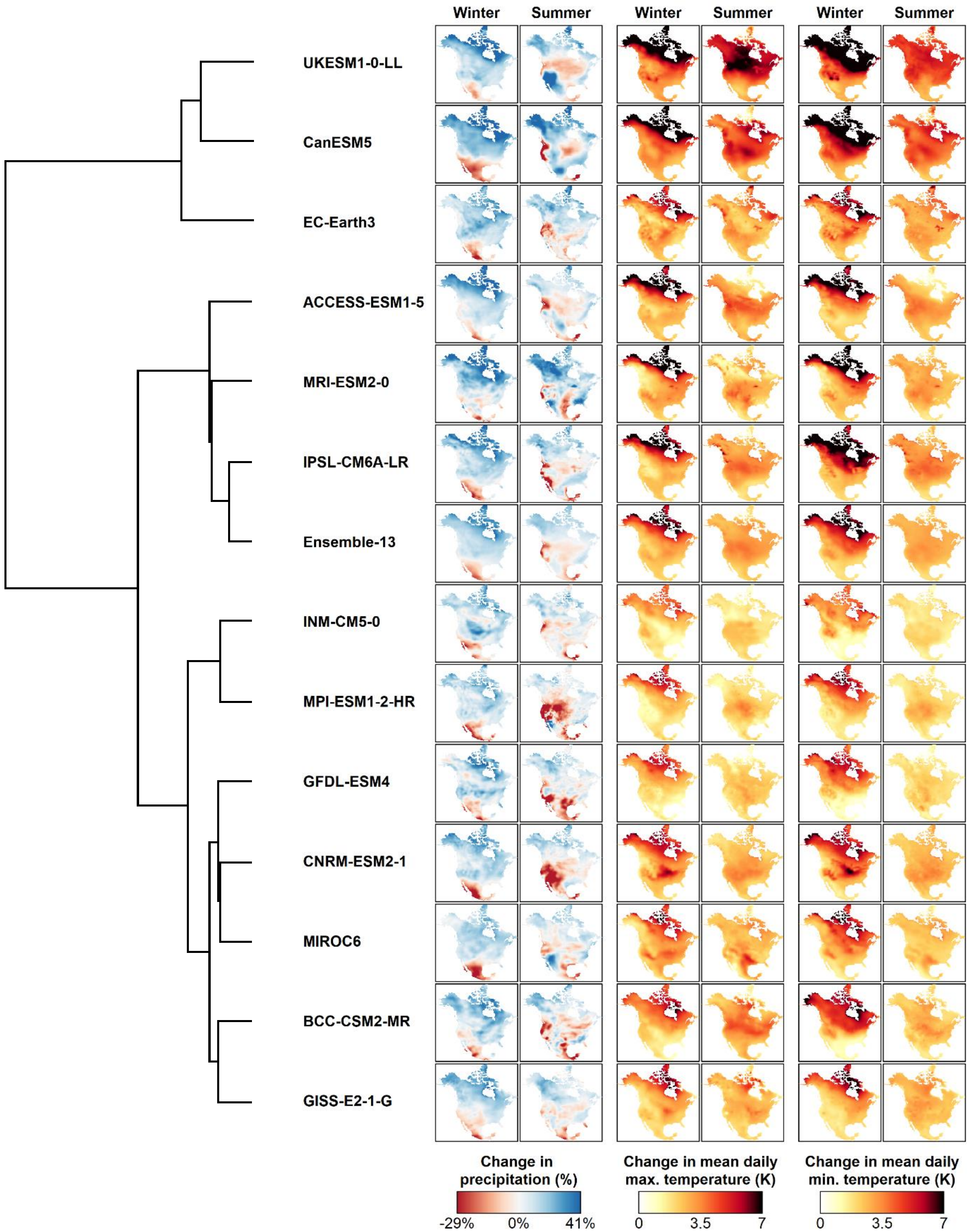

278 **Figure 3: Spatial variation in climate change responses among the 13-model ensemble.** Mapped climate changes are for the mean projected climate of the 2041-2060 period (SSP2-4.5). Precipitation is log-scaled to provide proportional magnitude of positive and negative changes. Models are structured by a cluster dendrogram of spatial similarity in seasonal climate changes in all three climate elements.

3.3. Ensemble subset selection

3.3.1. Screening Criteria

The following models are prioritized for exclusion from subsets of the ensemble based on combinations of the four screening criteria:

- CanESM5, because its very high climate sensitivity (ECS 5.6°C) is also represented by UKESM1-0-LL and because its very low horizontal resolution is less suitable for downscaling.

- INM-CM5-0, because it has very low climate sensitivity (ECS 1.9°C) and is an outlier among CMIP6 models for under-representing the observed 1975-2014 global temperature trend (Liang et al. 2020) (Criterion 7). In addition, this model has only one simulation for most scenarios, producing a less robust climate signal (Criterion 9).

- BCC-CSM2-MR, due to having a single simulation for each scenario (Criterion 9) and low topographic resolution (Criterion 8).

- IPSL-CM6A-LR, due to isolated grid cells with very high summer warming in the BC Coast Ranges and Southeast Alaska (Figure 4) (Criterion 10). The warming in these cells may be physically plausible in the model's simplified topography, but is problematic for downscaling to higher spatial resolutions.

A fifth model, UKESM1-0-LL, also has very high climate sensitivity, similar to CanESM5, that is assessed as very unlikely based on observational evidence (Sherwood et al. 2020, Tokarska et al. 2020). Some researchers may wish to constrain their ensemble subset to observations by excluding this model. Others may wish to include a high-sensitivity model in their subset as a representation of the long tail of uncertainty in the upper limit of climate sensitivity (Sutton 2018). To accommodate both perspectives, we provide structured subsets with and without UKESM1-0-LL in the ordered ensemble subsets. We preferred UKESM1-0-LL over CanESM5 as a representative of high-sensitivity models due to its higher grid resolution and closer alignment with the observed post-1970 global heating trend (Liang et al. 2020).

The 8-model subset has a mean global ECS of 3.4°C (2.6-4.8°C). The 9-model subset that includes UKESM1-0-LL has a mean global ECS of 3.6°C (2.6-5.4°C), using ECS values provided by Meehl et al. (2020).

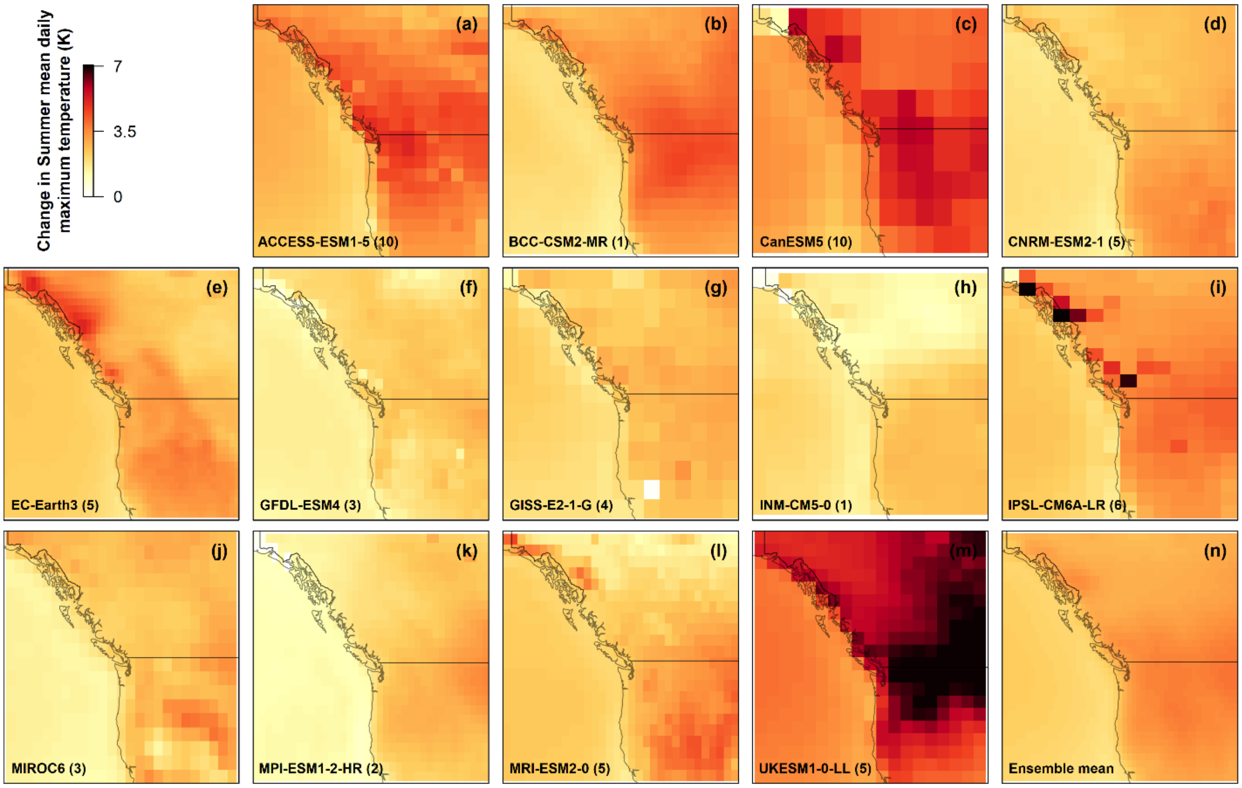

Figure 4: Summer daytime warming in the 13-model ensemble over central-western North America (106-142W, 37-62N). Values are the change in summer T_{max} for the 2041-2060 period (SSP2-4.5), relative to 1961-1990, in the native model grid. Change is calculated from the mean of multiple simulation runs per model, specified next to the model name.

3.3.2. Ordered subsets

Table 2 specifies ordered subsets of the 8-9 models that passed screening criteria 7-10. For a desired region and subset size, the ensemble subset for each region includes all models listed at and above the desired subset size. For example, a 4-model ensemble for the NEN region would include CNRM-ESM2-1, UKESM1-0-LL, EC-Earth3, and MPI-ESM1-2-HR. The considerable variation among regions in the order of the subsets underscores the spatial variation in climate change responses across North America. The exception to this variation in model order is that UKESM1-0-LL is the second model in all regions. Since the first position in the order is the model closest to the ensemble centroid and the second position is the model furthest from the centroid, this result indicates that UKESM1-0-LL consistently projects the most extreme climate changes throughout the continent.

Table 2: Ordered subsets of the 13-model ensemble. Subsets are provided for the 7 IPCC reference regions (Figure 5). Model abbreviations are ACC (ACCESS-ESM1-5), CNRM (CNRM-ESM2-1), EC (EC-Earth3), GFDL (GFDL-ESM4), GISS (GISS-E2-1-G), MIR (MIROC6), MPI (MPI-ESM1-2-HR), MRI (MRI-ESM2-0), and UK (UKESM1-0-LL). Exclusion of UKESM1-0-LL provides an ensemble that is consistent with assessed constraints on equilibrium climate sensitivity.

Subset	IPCC Reference Region						
size	**NEN**	**NWN**	**WNA**	**CNA**	**ENA**	**NCA**	**SCA**
Including UKESM1-0-LL							
1	CNRM	CNRM	MRI	ACC	EC	MRI	CNRM
2	UK	UK	UK	UK	UK	UK	UK
3	EC	MPI	MPI	MPI	MPI	GFDL	GFDL
4	MPI	EC	GISS	CNRM	MRI	MIR	ACC
5	MRI	ACC	MIR	MIR	MIR	EC	MPI
6	ACC	MRI	CNRM	GISS	GFDL	MPI	MIR
7	GFDL	MIR	GFDL	EC	ACC	CNRM	EC
8	GISS	GISS	EC	GFDL	GISS	ACC	GISS
9	MIR	GFDL	ACC	MRI	CNRM	GISS	MRI
Excluding UKESM1-0-LL							
1	CNRM	CNRM	MRI	MRI	GISS	GISS	CNRM
2	EC	EC	MPI	MPI	GFDL	EC	ACC
3	MPI	ACC	GISS	CNRM	MRI	MRI	GFDL
4	MRI	MPI	MIR	MIR	ACC	MIR	MPI
5	ACC	MIR	CNRM	EC	CNRM	GFDL	MIR
6	GISS	GISS	EC	GFDL	EC	CNRM	EC
7	GFDL	MRI	GFDL	GISS	MPI	ACC	GISS
8	MIR	GFDL	ACC	ACC	MIR	MPI	MRI

Figure 5: IPCC reference regions (Iturbide et al. 2020) used for region-specific ordered subsets of the ensemble.

4. Discussion

We selected 13 CMIP6 models from a candidate pool of 44 models contributing to the CMIP6 experiment. This 13-model ensemble is representative of the distribution of equilibrium climate sensitivity and grid resolution in ScenarioMIP. This ensemble facilitates robust downscaling by using multiple simulations per scenario for each model and excluding models with high bias. We provide rationale for a 9-member subset of the ensemble based on screening criteria and order these 9 models for selection of smaller ensembles for regional analysis in North America. With the exception of AWI-CM-1-1-MR, all models were excluded using global criteria. Consequently, the 13-member ensemble is a good starting point for downscaling climate normals in other Continents.

4.1. Model bias

The bias assessment was a useful way to identify models with extreme divergence from the observed climate. High biases were the sole basis for the exclusion of one model, AWI-CM1-1-1-MR, and are an attribute of concern in two of the models selected for the ensemble, ACCESS-ESM1-5 and MIROC6. Moderate biases, however, do not necessarily indicate a problem with the models. Bias is the difference between model simulations and the observed climate. We controlled the confounding influence of natural variability in each model by calculating bias using the mean of several simulation runs. This measure is not possible for observations since there is only one realization of the observed climate. Natural variability in the observed climate, therefore, could produce apparent biases even in a hypothetical "perfect" model. The ensemble mean absolute bias of 2^{o}C in temperature and by a factor of 1.5 in precipitation cannot be definitively attributed to the models or the ensemble; it is to some extent an artefact of natural variability in the observed climate.

4.2. Grid resolution

Four of the models in the ensemble have horizontal grid resolution sufficient to resolve major mountain ranges. One model (EC-Earth3) has relatively high resolution (0.7^{o}x0.7^{o}) approaching the previous generation of regional climate models used for dynamical downscaling. The trend towards higher resolution is encouraging, but the benefits of moderate resolution models for km-scale downscaling are ambiguous. On one hand, resolving mountain ranges allows for stronger differentiation of coast-interior transitions, windward and leeward dynamics, and elevation-dependent climate changes. On the other hand, these resolved ranges are still highly simplified features. Resolved high-elevation processes such as enhanced warming due to snow albedo feedbacks will be applied to unresolved low-elevation locations (e.g. valleys) during change-factor downscaling. While solving some of the problems of lower-resolution models, higher-resolution models introduce new problems. In the absence of additional statistical downscaling measures to address these problems, we do not view the higher-resolution models in the ensemble as intrinsically more valuable or valid. They do, however, make a distinct contribution and the range of grid resolution in the ensemble improves the representation of modeling uncertainties.

5. Acknowledgements

We acknowledge the World Climate Research Programme, which, through its Working Group on Coupled Modelling, coordinated and promoted CMIP6. We thank the climate modeling groups for producing and making available their model output, the Earth System Grid Federation (ESGF) for archiving the data and providing access, and the multiple funding agencies who support CMIP6 and ESGF.

6. Literature Cited

Brunner, L., R. Lorenz, M. Zumwald, and R. Knutti. 2019. Quantifying uncertainty in European climate projections using combined performance-independence weighting. Environmental Research Letters 14:124010.

Cannon, A. J. 2015. Selecting GCM scenarios that span the range of changes in a multimodel ensemble: Application to CMIP5 climate extremes indices. Journal of Climate 28:1260–1267.

Cannon, A. J. 2018. Multivariate quantile mapping bias correction: an N-dimensional probability density function transform for climate model simulations of multiple variables. Climate Dynamics 50:31–49.

Eyring, V., S. Bony, G. A. Meehl, C. A. Senior, B. Stevens, R. J. Stouffer, and K. E. Taylor. 2016. Overview of the Coupled Model Intercomparison Project Phase 6 (CMIP6) experimental design and organization. Geoscientific Model Development 9:1937–1958.

Fick, S. E., and R. J. Hijmans. 2017. WorldClim 2: new 1-km spatial resolution climate surfaces for global land areas. International Journal of Climatology 37:4302–4315.

Hamann, A., T. Wang, D. L. Spittlehouse, and T. Q. Murdock. 2013. A comprehensive, high-resolution database of historical and projected climate surfaces for western North America. Bulletin of the American Meteorological Society 94:1307–1309.

Hijmans, R. J., S. E. Cameron, J. L. Parra, P. G. Jones, and A. Jarvis. 2005. Very high resolution interpolated climate surfaces for global land areas. International Journal of Climatology 25:1965–1978.

Iturbide, M., J. M. Gutiérrez, L. M. Alves, J. Bedia, R. Cerezo-Mota, E. Cimadevilla, A. S. Cofiño, A. Di Luca, S. H. Faria, I. V. Gorodetskaya, M. Hauser, S. Herrera, K. Hennessy, H. T. Hewitt, R. G. Jones, S. Krakovska, R. Manzanas, D. Martínez-Castro, G. T. Narisma, I. S. Nurhati, I. Pinto, S. I. Seneviratne, B. van den Hurk, and C. S. Vera. 2020. An update of IPCC climate reference regions for subcontinental analysis of climate model data: definition and aggregated datasets. Earth System Science Data 12:2959–2970.

Leduc, M., R. Laprise, R. de Elia, and L. Separovic. 2016. Is Institutional Democracy a Good Proxy for Model Independence? Journal of Climate 29:8301–8316.

Liang, Y., N. P. Gillett, and A. H. Monahan. 2020. Climate Model Projections of 21st Century Global Warming Constrained Using the Observed Warming Trend. Geophysical Research Letters 47:1–10.

Maraun, D. 2016. Bias Correcting Climate Change Simulations - a Critical Review. Current Climate Change Reports 2:211–220.

McSweeney, C. F., R. G. Jones, R. W. Lee, and D. P. Rowell. 2014. Selecting CMIP5 GCMs for downscaling over multiple regions. Climate Dynamics 44:3237–3260.

Meehl, G. A., C. A. Senior, V. Eyring, G. Flato, J. F. Lamarque, R. J. Stouffer, K. E. Taylor, and M. Schlund. 2020. Context for interpreting equilibrium climate sensitivity and transient climate response from the CMIP6 Earth system models. Science Advances 6:1–11.

Palazzi, E., L. Mortarini, S. Terzago, and J. von Hardenberg. 2019. Elevation-dependent warming in global climate model simulations at high spatial resolution. Climate Dynamics 52:2685–2702.

Pierce, D. W., T. P. Barnett, B. D. Santer, and P. J. Gleckler. 2009. Selecting global climate models for regional climate change studies. Proceedings of the National Academy of Sciences of the United States of America 106:8441–8446.

Sherwood, S., M. J. Webb, J. D. Annan, K. C. Armour, P. M. Forster, J. C. Hargreaves, G. Hegerl, S. A. Klein, K. D. Marvel, E. J. Rohling, M. Watanabe, T. Andrews, P. Braconnot, C. S. Bretherton, G. L. Foster, Z. Hausfather, A. S. von der Heydt, R. Knutti, T. Mauritsen, J. R. Norris, C. Proistosescu, M. Rugenstein, G. A. Schmidt, K. B. Tokarska, and M. D. Zelinka. 2020. An assessment of Earth’s climate sensitivity using multiple lines of evidence. Reviews of Geophysics:0–2.

Sutton, R. T. 2018. ESD Ideas: A simple proposal to improve the contribution of IPCC WGI to the assessment and communication of climate change risks. Earth System Dynamics 9:1155–1158.

Sutton, R. T., and E. Hawkins. 2020. ESD Ideas : Global climate response scenarios for IPCC assessments:751–754.

Tabor, K., and J. W. Williams. 2010. Globally downscaled climate projections for assessing the conservation impacts of climate change. Ecological Applications 20:554–565.

Taylor, K. E., R. J. Stouffer, and G. A. Meehl. 2012. An overview of CMIP5 and the experiment design. Bulletin of the American Meteorological Society 93:485–498.

Tokarska, K. B., M. B. Stolpe, S. Sippel, E. M. Fischer, C. J. Smith, F. Lehner, and R. Knutti. 2020. Past warming trend constrains future warming in CMIP6 models. Science Advances 6:eaaz9549.

Wang, T., A. Hamann, D. Spittlehouse, and C. Carroll. 2016. Locally downscaled and spatially customizable climate data for historical and future periods for North America. Plos One 11:e0156720.

Wang, T., A. Hamann, D. L. Spittlehouse, and T. Q. Murdock. 2012. ClimateWNA: high-resolution spatial climate data for western North America. Journal of Applied Meteorology and Climatology 51:16–29.

Wilby, R. L., S. P. Charles, E. Zorita, B. Timbal, P. Whetton, and L. O. Mearns. 2004. Guidelines for Use of Climate Scenarios Developed from Statistical Downscaling Methods. IPCC Task Group on Data and Scenario Support for Impact and Climate Analysis (TGICA).